Materials and methods:

Patient samples. Metastatic melanoma samples were obtained from patients who received ipilimumab as the standard of care. Prostate cancer samples were obtained from a phase II study of androgen deprivation therapy in combination with ipilimumab from metastatic non-castrate disease in patients who received androgen deprivation therapy within 1 month of starting ipilimumab (#NCT01377389). Samples were collected at baseline (before patients started ipilimumab) and after three of ipilimumab.

Mice. C57BL/6 (5–7 weeks) mice were purchased from the National Cancer Institute (Frederick, MD). *FoxP3*^{cre}, *EZH2*$^{fl/fl}$, *FoxP3*-eGFP, and *Rag1*$^{-/-}$ mice (5-7 weeks old), all of the C57BL/6 background, were obtained from The Jackson Laboratory (Bar Harbor, ME). *FoxP3*^{cre}*EZH2*$^{fl/fl}$ mice were generated by breeding FoxP3^{cre} and EZH2$^{fl/fl}$ C57BL/6 mice. All mice were kept in specific pathogen-free conditions in the Animal Resource Center at The University of Texas MD Anderson Cancer Center. Animal protocols were approved by the Institutional Animal Care and Use Committee of The University of Texas MD Anderson Cancer Center.

Cell lines and tumor model. Murine bladder cancer cell line (MB49) were provided by Dr. A. Kamat (at The University of Texas MD Anderson Cancer Center, Houston, TX) and murine melanoma cell line B16-F10 was obtained from Dr. I. Fidler (The University of Texas MD Anderson Cancer Center, Houston, TX) (1, 2). 2 X 10^5 (MB49) or 2 X 10^5 (B16-F10) cells were injected subcutaneously or intradermally respectively, in the right flanks of C57BL/6 mice (5 or 10 mice per group). EZH2 inhibitor (CPI-1205; Constellation Pharmaceuticals Cambridge, MA) (200 mg/kg) was administered twice daily through oral

gavage from day 3 to the end of the experiment. On day 7 after tumor inoculation, when tumors became palpable, mice were injected intraperitoneally with α-CTLA-4 (clone 9H10, Bio X Cell, NH, catalog number BE0131) (100 μg/mouse). A second dose of anti–CTLA-4 was administered on day 9.

Tissue processing and flow cytometry. Tumor bearing mice were sacrificed on day 14 and single cell suspensions from spleen, lymph node and tumor were prepared as described previously (3). Single cell suspension from frozen human peripheral blood samples were performed as described previously (4). For flow cytometry based analysis of surface markers, cells were stained in phosphate-buffered saline containing 5% bovine serum albumin with LIVE/DEAD yellow dye (Thermo Fisher Scientific catalog number L34959), anti-CD45 (Biolegend, 30-F11), anti-CD4 (BioLegend, RM4-5), anti-CD8α (BioLegend, 53-6.7), anti-CD44 (eBioscience, 1M7), anti-CD62L (BioLegend, MEL-14), anti-CD25 (BioLegend, 3C7), anti-ICOS (eBioscience, 7E.17G9), anti-CD27 (eBioscience, LG.7F9), anti-CD39 (eBioscience, 24DMS1), anti-FR4 (eBioscience, eBio12A5), CD4 (BioLegend, OKT4), CD25 (BioLegend, M-A251), FoxP3 (eBioscience, 236A/E7), anti-CD3 (BioLegend, UCHT1), anti-CD8a (BioLegend, RPA-T8), anti-CD25 (BioLegend, BC96), anti-CD197 (BioLegend, CCR7), anti-CD45RA (BioLegend, HI100), and anti-CD45RO (BioLegend, UCHL1) on ice for 30 minutes. Staining with intracellular anti-Foxp3 (eBioscience, FJK-16 s), anti–IL-2 (eBioscience, PC61.5), anti–Ki-67 (eBioscience, SolA15), anti–IFN-γ (BioLegend, XMG1.2), anti-TNF-α (BioLegend, MP6-XT22), and anti-EZH2 (Cell Signaling Technology, D2C9) were analyzed by flow cytometry according to the manufacturers' instructions. Flow cytometry data were

acquired on BD LSR II (BD Biosciences) and analyzed using FlowJo software V10 (Tree Star, Ashland, OR).

In vitro T cell assays. Human peripheral regulatory T cells were isolated from peripheral blood mononuclear cells by enriching for $CD4^+CD127^{low}CD25^+$ cells using the EasySep Human Regulatory T Cell Isolation Kit (STEMCELL Technologies, Cambridge, MA). For mouse in vitro regulatory T cell differentiation, $CD4^+CD25^{low}CD44^{low}CD62L^{hi}$ naïve splenic T cells were isolated from C57BL/6 mice using BD FACSAria (BD Biosciences, San Jose, CA). The cells were then differentiated in the presence of recombinant murine IL-2 (R&D, 402-ML), tumor growth factor-β (TGF-β, R&D 7666-MB), CPI-1205 or dimethyl sulfoxide (DMSO) and cultured for 6 days.

For T cell suppression assays, autologous $CD4^+$ conventional T cells (Tconv) were isolated by magnetic separation (STEMCELL Technologies) from cryopreserved peripheral blood mononuclear cells rested overnight. Tconv were labeled with CellTrace Violet (Thermo Fisher Scientific, Waltham, MA) as instructed by the manufacturer. Tconv and autologous induced regulatory T cells were co-cultured in various ratios in ImmunoCult medium (STEMCELL Technologies). Suppression was subsequently analyzed by flow cytometry (CellTrace Violet–based proliferation in combination with fixable live/dead dye and CD4, CD25, and FOXP3 staining).

T cell cytotoxicity assay was carried out using activated effector T cells (isolated with EasySep Human Naive $CD4^+$ T Cell Isolation Kit and EasySep Human $CD8^+$ T Cell Enrichment Kit; STEMCELL Technologies). Purified naive CD4 and total CD8 T cells were pre-activated with plate-bound anti-CD3/soluble anti-CD28 for 6 days in the presence or

absence of CPI-1205. Activated T cells were then washed and challenged with Nalm-6 target tumor cells, then labeled with CellTrace violet to enable their subsequent discrimination from effector cells. The T cell:tumor cell co-cultures were conducted at different effector:target (E:T) ratios, in the presence of the blinatumomab antibody (10ng/ml) and CPI-1205 for 20 hours as previously described (5).Target cell death was determined by summing the percentage of apoptotic (Annexin V^+) and dead or dying ($7AAD^+$) target (CellTrace $violet^+$) cells after overnight culture.

RNA sequencing. RNA was extracted from peripheral CD4 T cells isolated from patients with metastatic melanoma and from in vitro differentiated GFP^+ regulatory T cells. RNA sequencing reactions were performed by Active Motif (Carlsbad, CA) and Ocean Ridge Biosciences (Deerfield, FL) using an Illumina HiSeq 50-bp platform. For bioinformatics analysis, the raw reads were aligned to the mm10 reference genome using TopHat2. HTSeq count was used to count the raw reads that were uniquely mapped to each gene. DESeq2 was then applied to normalize the raw read counts and identify the differentially expressed genes between the groups. The beta-uniform mixture model was used to fit the p value distribution for multiple testing adjustments. The lists of differentially expressed genes were then used as input into Ingenuity Pathway Analysis for pathway analysis.

Quantitative Real-time RT–PCR. RNA is extracted using RNeasy Plus Micro Kit (QIAGEN) and reverse-transcription reactions were performed using miScript II RT Kit (QIAGEN), RT-PCR was performed using 7500 Fast Real-time PCR System (Applied Biosystems). The specific primers (origene) used for the assays are listed below.

Primer sequences:

Actin (F : CATTGCTGACAGGATGCAGAAGG, R: TGCTGGAAGGTGGACAGTGAGG)

CXCL9(F:CCTAGTGATAAGGAATGCACGATG,R: CTAGGCAGGTTTGATCTCCGTTC)

CXCL10(F: ATCATCCCTGCGAGCCTATCCT, R: GACCTTTTTTGGCTAAACGCTTTC)

Western blot. Cell lysates were prepared from mouse CD4 and CD8 T cells, Western blot was performed using a standard Western blot protocol with EZH2 (Cell Signaling Technology, D2C9). Quantitation was performed using LI-COR Biosciences (Lincoln, NE) Image Studio software.

Statistical analysis. All data are representative of at least two to three independent experiments with 5–10 mice in each in vivo experiment . The data are expressed as mean ± standard error of the mean (SEM) and were analyzed using Prism 5.0 statistical analysis software (GraphPad Software, La Jolla, CA). Student t-tests (two tailed), ANOVA, and Bonferroni multiple comparison tests were used to identify significant differences ($p<0.05$) between treatment groups. Ingenuity Pathway Analysis was done on data obtained from RNA sequencing using Ingenuity Pathway Analysis software (QIAGEN, Hilden, Germany).

Supplemental figures:

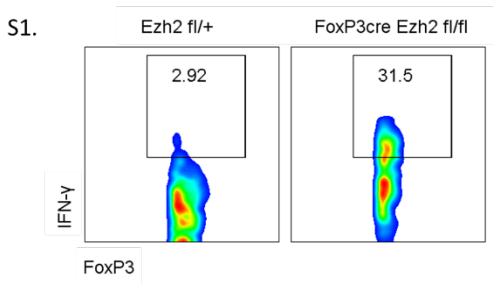

Figure S1. Flow plot depicting percentages of intra-tumoral FoxP3^{+}IFNγ^{+} cells in MB49 tumor-bearing *EZH2$^{fl/+}$* (n=10) and *FoxP3^{Cre}EZH2$^{fl/fl}$* (n=10) mice. Data are representative of three independent experiments. (2 tailed student t test was used to determine significance; **p<0.01).

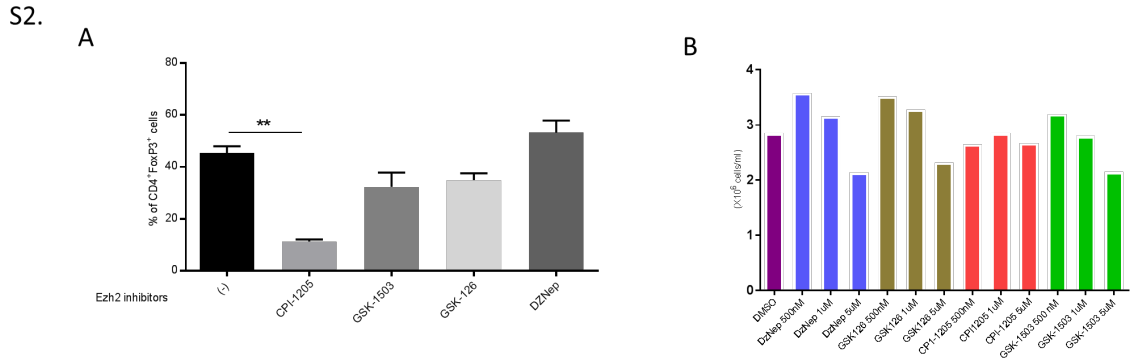

Figure S2. (A) Percentages of inducible regulatory T cells following in vitro differentiation of murine naive CD4 T cells into regulatory T cells in the presence and absence of various EZH2 inhibitors. (B) Representative counts of viable cells in culture following treatment with EZH2 inhibitors. Data are representative of three independent experiments. (One-way ANOVA was used to determine significance between the groups. **p<0.01).

S3.

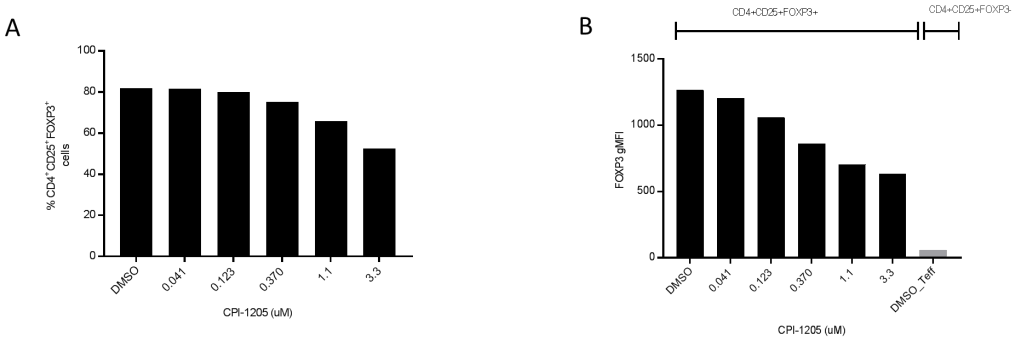

Figure S3. Human PBMC derived T cells were differentiated to $CD4^+CD25^+FoxP3^+$ cells at different doses of CPI-1205. Representative bar graphs depict (A) percentage of $CD4^+CD25^+FoxP3^+$ cells and (B) Mean Fluorescent Intensity (MFI) of FoxP3 expression of these cells. Data are representative of three independent experiments.

S4.

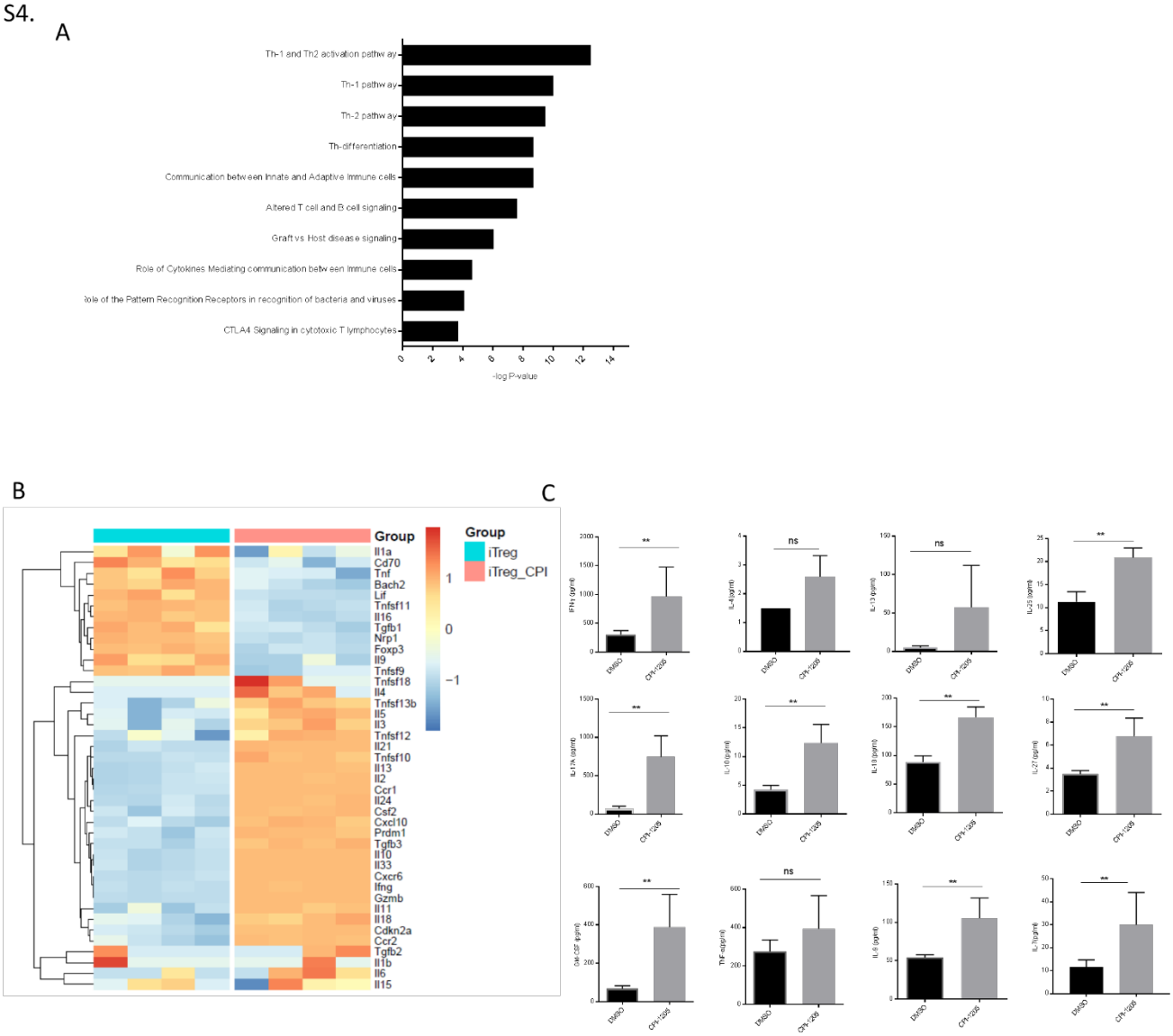

Figure S4. Naïve T cells from FoxP3–enhanced green fluorescent protein (eGFP) C57BL/6 mice that were differentiated into iTregs in the presence or absence of CPI-1205. GFP^{+}FoxP3^{+} regulatory T cells were subsequently used for RNA sequencing analysis. (A) Ingenuity Pathway Analysis of RNA sequencing data of regulatory T cells differentiated in the presence of DMSO or CPI-1205. (B) Differentially expressed genes (DEGs) seen following differentiation of inducible regulatory T cells in presence of CPI-1205 or DMSO. (C) Luminex-based cytokine analysis of culture supernatant from inducible regulatory T cells following differentiation with CPI-1205 or DMSO. (2 tailed student t test was used to determine significance; NS, not significant. **p<0.01).

S5.

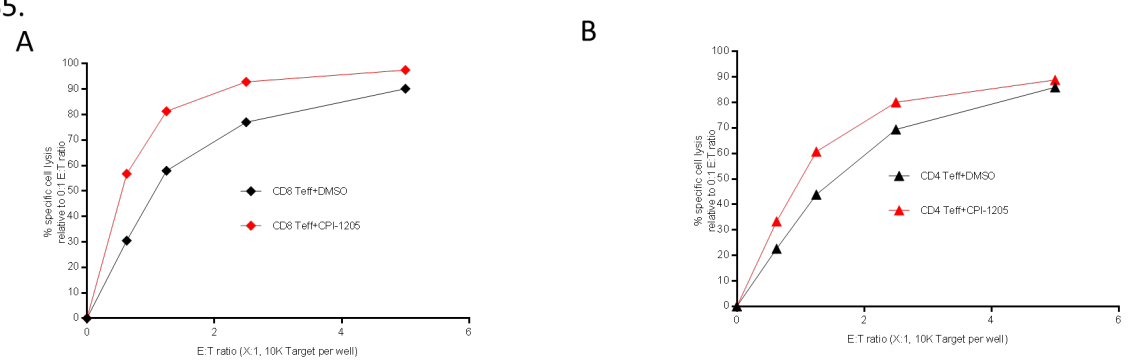

Figure S5. Pre-activated human CD4 and CD8 T cells (+/- CPI-1205) were cultured with CellTrace Violet–labeled Nalm-6 target cells along with blinatumomab. Data is presented as % specific cell lysis at various ratios of effector:target cells. Data are representative of three independent experiments. (2 tailed student t test was used to determine significance; **p<0.01).

S6.

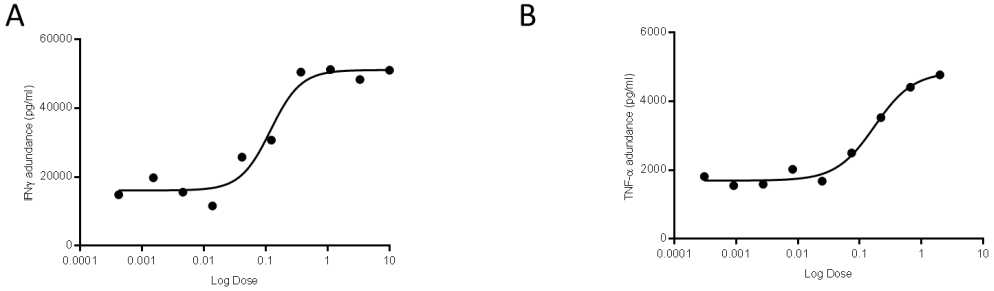

Figure S6. Abundance of IFNγ (A) and TNFα (B) measured by Meso Scale Diagnostics enzyme-linked immunosorbent assay (MSD-ELISA) in the supernatant of human CD4 T cells following stimulation with anti-CD3 and anti-CD28 at various doses of CPI-1205. Data are representative of two independent experiments with IC50 of 0.123 ± 0.005 and 0.155 ± 0.027 uM for IFNγ and TNFα, respectively.

S7. A

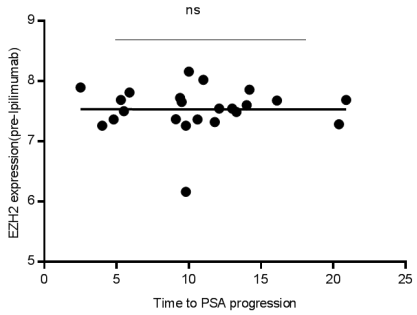

B

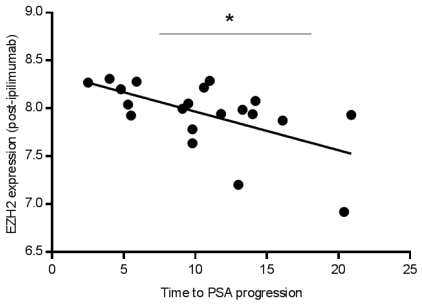

Figure S7. EZH2 expression in $CD4^+$ cells at baseline (A) and after ipilimumab therapy (B) correlated with time to prostate-specific antigen progression by Spearman correlation (*p<0.05). NS, not significant.

S8.

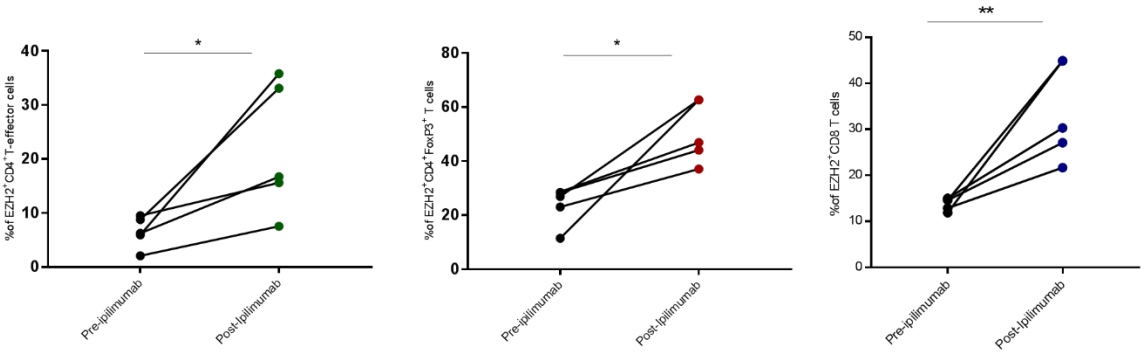

Figure S8. Flow cytometry analysis of EZH2 expression on $CD4^+CD45RO^-$ $CD45RA^+CCR7^-$ (CD4 T effector, Teff), $CD4^+CD25^+FoxP3^+$ (T regulatory, T-reg) and CD8 T cells derived from peripheral blood mononuclear cells of patients with metastatic melanoma at baseline and after three doses of ipilimumab. Matched pair analysis of EZH2 expression before and after ipilimumab therapy. (Student t-test was used to determinesignificance. **p<0.01, *p<0.05).

S9.

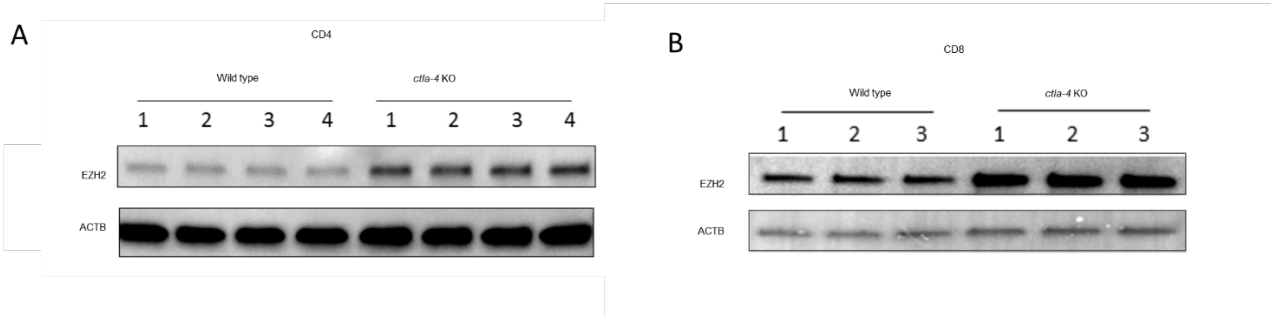

Figure S9. Western blot analysis of CD4 and CD8 T cells derived from the spleen and lymph node of CTLA-4$^{-/-}$ mice and wild-type (WT) littermate controls. Data are representative of three independent experiments

S10.

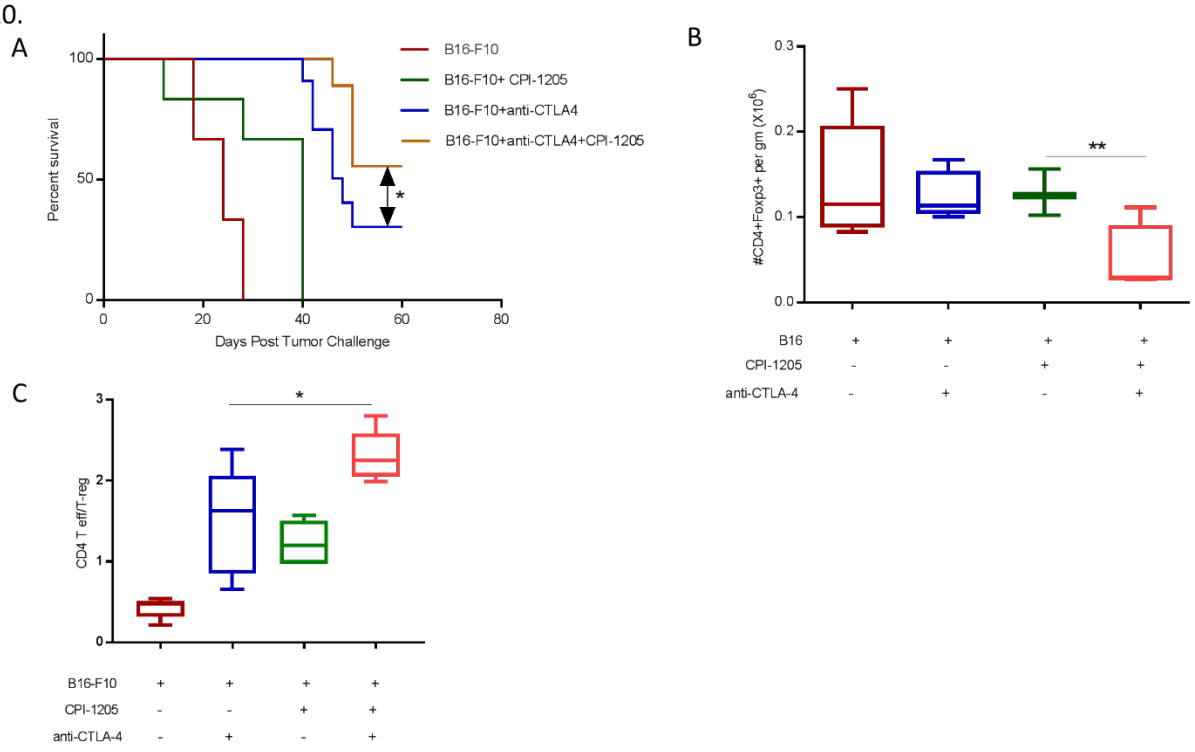

Figure S10. (A) Survival curve from representative experiments of B16-F10 tumor-bearing mice treated with vehicle, anti–CTLA-4, CPI-1205, or the combination of anti–CTLA-4 and CPI-1205. (B) Absolute numbers of intra-tumoral CD4^{+}FoxP3^{+} regulatory T cells and (C) Ratio of CD4 T-effector cells and regulatory T cells from B16-F10 tumor-

bearing mice treated with vehicle, anti–CTLA-4, CPI-1205, or the combination of anti–CTLA-4 and CPI-1205. Data are representative of two independent experiments. (n=10 in each group, **p<0.01).

S11.

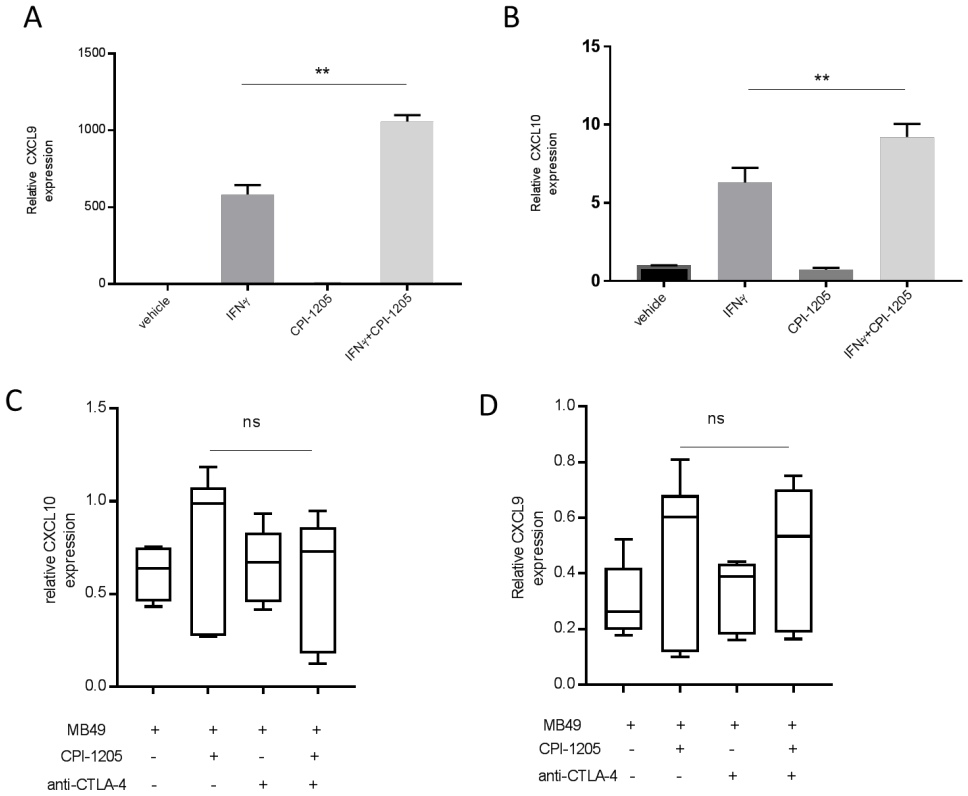

Figure S11. (A-B) Real-time RT-PCR analysis of CXCL9 and CXCL10 in B16-F10 and MB-49 cell lines following stimulation with vehicle, IFNγ, CPI-1205 or combination of IFNγ and CPI-1205 presented relative to the expression of actin. (C-D) Relative CXCL9 and CXCL10 expression in the tumor following treatment with vehicle, anti–CTLA-4, CPI-1205, or the combination of anti–CTLA-4 and CPI-1205 in MB49 tumor-bearing mice. Data are representative of two independent experiments. (n=5 in each group. One-way ANOVA was used for significance. **p<0.01, *p<0.05). NS, not significant.

References

1. Summerhayes IC, and Franks LM. Effects of donor age on neoplastic transformation of adult mouse bladder epithelium in vitro. *J Natl Cancer Inst.* 1979;62(4):1017-23.
2. Fidler IJ. Selection of successive tumour lines for metastasis. *Nat New Biol.* 1973;242(118):148-9.
3. Simpson TR, Li F, Montalvo-Ortiz W, Sepulveda MA, Bergerhoff K, Arce F, Roddie C, Henry JY, Yagita H, Wolchok JD, et al. Fc-dependent depletion of tumor-infiltrating regulatory T cells co-defines the efficacy of anti-CTLA-4 therapy against melanoma. *The Journal of experimental medicine.* 2013;210(9):1695-710.
4. Ng Tang D, Shen Y, Sun J, Wen S, Wolchok JD, Yuan J, Allison JP, and Sharma P. Increased frequency of ICOS+ CD4 T cells as a pharmacodynamic biomarker for anti-CTLA-4 therapy. *Cancer immunology research.* 2013;1(4):229-34.
5. Molhoj M, Crommer S, Brischwein K, Rau D, Sriskandarajah M, Hoffmann P, Kufer P, Hofmeister R, and Baeuerle PA. CD19-/CD3-bispecific antibody of the BiTE class is far superior to tandem diabody with respect to redirected tumor cell lysis. *Mol Immunol.* 2007;44(8):1935-43.